JOURNAL OF CATALYSIS **175,** 269–279 (1998)
ARTICLE NO. CA981999

Reduction of NO by CO over $Rh/CeO_2–ZrO_2$ Catalysts

Evidence for a Support-Promoted Catalytic Activity

P. Fornasiero,* G. Ranga Rao,† J. Kašpar,*,[1] F. L'Erario,* and M. Graziani*

**Dipartimento di Scienze Chimiche, Università di Trieste, Via Giorgieri 1, 34127 Trieste, Italy; and †Catalysis Section, Department of Chemistry, Indian Institute of Technology, Madras 600 036, India*

Received September 23, 1997; revised November 13, 1997; accepted December 22, 1997

Reduction of NO by CO catalysed by $Rh/CeO_2–ZrO_2$ solid solutions is investigated with the aim to elucidate the role of the $CeO_2–ZrO_2$ supports in modifying the activity of supported Rh. Two distinct kinetic regimes, characterised by different activation energies are observed below and above 500 K. It is proposed that below 500 K the reduction of NO occurs at the expenses of a concomitant oxidation of Ce^{3+} sites. In this model, the supported metal activates the reducing agent favouring the efficiency of Ce^{4+}/Ce^{3+} redox couple. The influence of a high temperature reduction (H_2, 1073 K) is also investigated. Such a treatment, which increases the reducibility at low temperatures of the $CeO_2–ZrO_2$ solid solution, promotes the efficiency of the catalysts at low temperatures, confirming the important role of the Ce^{4+}/Ce^{3+} redox couple in determining the activity of the catalyst.

Key Words: **exhaust catalysts; rhodium; $CeO_2–ZrO_2$ solid solutions; $CeO_2–ZrO_2$ mixed oxides; NO reduction; CO oxidation; oxygen storage; temperature programmed reduction; redox properties.**

INTRODUCTION

NO reduction by CO is a key step in the catalytic control of automotive exhaust. This reaction is responsible for the removal of NO from the exhaust and it contributes to the elimination of CO as well. Rhodium is added to the commercial three-way catalysts (TWCs) due to its ability to specifically enhance the NO conversion (1, 2). The high activity of rhodium for NO removal is associated with its ability to efficiently dissociate NO (1, 3). Due to the high cost of rhodium, an increase in efficiency or use of substitutes is of strong interest. Among the other components of the TWCs, CeO_2 deserves a particular attention since multiple promoting effects were ascribed to this component (1, 3, 4): (i) oxygen storage/release capacity; (ii) stabilisation of noble metal dispersion; (iii) promotion of the water gas shift reaction. In addition to these properties, laboratory studies showed that ceria favourably alters the kinetics of the NO–CO reaction (5). Therefore, the investigation of the metal-ceria interactions induced effects on the conversions of the exhaust is receiving much interest in the literature. Short lived, but highly productive, enhancement of the conversion have been observed over ceria containing TWCs after a reductive pretreatment (6). Typically, after such a treatment, light-off temperatures, e.g. 50% conversion of CO and hydrocarbons (HC), are lowered by 50–100 K (7). Significantly, also the NO_x conversion was enhanced by such a reductive pretreatment. Either formation of highly active sites at the interface between the metal and the reduced CeO_2 or generation of a new active phase formed by migration of the metal into the ceria lattice have been suggested to be responsible for this phenomenon. Recently, metal covering by ceria particles has also been invoked (6).

It is noteworthy that all the investigations underline the essential role of the reduced ceria in the formation of the active catalyst. Recently, we showed that incorporation of ZrO_2 into the CeO_2 lattice strongly promotes the reducibility of metal-loaded mixed ceria–zirconia oxides (8). Moreover, we observed that on the reduced support, NO decomposition promptly occurs (9, 10). This observation makes the investigation of the catalytic properties of the metal-loaded $CeO_2–ZrO_2$ catalysts of strong interest. It should be noted, however, that in the previous studies (9, 10) only low surface area samples were investigated, but for catalytic applications, high surface area of the support is desirable. The investigation of the reduction/oxidation behaviour of high surface area $Ce_{0.5}Zr_{0.5}O_2$ disclosed an unusual promotion of the redox behaviour upon repetitive reduction/oxidation of the solid solution (11, 12). In the present paper the catalytic behaviour of high surface area Rh-loaded $CeO_2–ZrO_2$ is addressed. The kinetics of the reaction of NO by CO is examined with the aim of elucidating the role of the support in promoting the activity of the supported Rh. Favourable effects of CeO_2 on the kinetics of this reaction and evidence for a support involving mechanism have been reported. In view of the previous observation of the effects of a high temperature reduction

[1] Corresponding author. E-mail: kaspar@univ.trieste.it.

0021-9517/98 $25.00

on the redox properties of the $Ce_{0.5}Zr_{0.5}O_2$, the influence of such treatment on the catalytic properties is also investigated.

EXPERIMENTAL

Solid $Ce_xZr_{1-x}O_2$ (x = 0.4–0.6) solutions were synthesised by a homogeneous gel route from $Ce(acac)_4$ and $Zr(O{-}Bu)_4$ precursors (Aldrich), according to previous reports (13, 14). The support was calcined at 773 K for 5 h and then impregnated by the incipient wetness method with a solution of $RhCl_3 \cdot nH_2O$ to obtain a Rh nominal loading of 0.5 wt%, afterwards the catalyst was dried at 393 K overnight and calcined at 773 K for 5 h. Hereafter these samples are designated as "fresh" ones. 0.5 wt% Rh/Al_2O_3 and Rh/CeO_2 were from previous studies (14, 15).

H_2 chemisorption was carried out at 233 K on a Micromeritics ASAP 2000 instrument. The adsorption isotherm was measured in the pressure range 100–400 Torr of H_2 and the amount of H_2 adsorbed was evaluated by extrapolation of the linear part of the isotherm back to zero pressure.

Catalytic experiments were carried out in differential conditions using a U-shaped quartz micro reactor (NO (1%) and CO (1–3%) in He, total flow 30 ml min^{-1}, GHSV = 12500–50000 h^{-1}). Typically 0.04–0.08 g of the catalyst were loaded between two layers of granular quartz which acted as a preheater. Reaction temperature was monitored by means of a thermocouple located in the catalyst bed. The absence of diffusional limitations was checked. Before the activity measurements, the fresh catalysts were reduced at 473 or 1073 K in H_2 (20 ml min^{-1}) for 2 h; H_2 was desorbed at the reduction temperature in He flow for 2 h. The effluents of the reactor (NO, N_2, N_2O, CO, and CO_2) were analysed by an on-line Hewlett–Packard 5890 II gaschromatograph equipped with a thermal conductivity detector. Presence of O_2 in the effluents can be detected at ppm level. The separation of the gaseous mixture, including O_2, was achieved by employing Hayesep A and Porapak Q columns. Research grade purity gas mixtures (>99.997%) were employed without further purification. GLC analysis showed the presence of traces of N_2O and N_2 in the feed mixture which have been taken into account in the conversion measurements. Temperature-programmed oxidation (TPO) and reduction (TPR (CO)) experiments using NO and CO as oxidant and reductant, respectively, were carried in flow of NO or CO (1% in He, 30 ml min^{-1}) at a heating rate of 1 K min^{-1} using the same equipment employed for the catalytic measurements.

X-ray absorption near edge spectroscopy (XANES) measurements were carried out at the EXAFS-I station on the DCI accumulation ring (energy 1.85 GeV, current 300 mV) at LURE (Orsay, France). The spectra were collected in the transmission mode, in the range of energies 5670–5790 eV and at a resolution of 0.3 eV. A channel-cut Si 331 monochromator was employed and the ionisation chambers were filled with air. Absence of any contribution to the spectrum of photons due to the third harmonic was accurately checked. Preedge background was linearly fitted in the region 5680–5710 eV, and this contribution was then subtracted from the experimental spectrum. All spectra were normalised to 1 at energy of 5790 eV. A thin film (5–7 mg cm^{-2}) of the catalyst was deposited onto a graphite holder from an acetone suspension, which was then inserted in an *in situ* XANES cell.

In situ IR spectra were recorded on a Perkin Elmer FT 2000 spectrometer as reported previously (15).

RESULTS

Description of the Fresh Metal-Free and Rh-Loaded $Ce_xZr_{1-x}O_2$ (x = 0.4–0.6)

The $Ce_xZr_{1-x}O_2$ (x = 0.4, 0.5, and 0.6) samples employed in the present work feature respectively surface areas of 76, 64, and 60 m^2 g^{-1}. XRD and Raman characterisation suggested the attribution of the samples to t'' phase following the classification proposed by Yashima *et al.* (16) even if the presence of t' phase in the case of the $Ce_{0.4}Zr_{0.6}O_2$ cannot be excluded due to the broadness of the XRD peaks. The t'' phase is characterised by a cation sublattice of Fm3m cubic symmetry, while the oxygen anions are displaced from their ideal fluorite sites. Upon impregnation with $RhCl_3 \cdot nH_2O$ and subsequent calcination, no significant structural modification of the support could be detected while the surface area decreased to 53 m^2 g^{-1} in the case of the $Rh/Ce_{0.5}Zr_{0.5}O_2$ (14).

H/Rh values of 0.27 and 0.20 were measured for the $Rh/Ce_{0.5}Zr_{0.5}O_2$ by H_2 chemisorption at 233 K respectively after reduction at 473 and 1000 K. As shown by Bernal *et al.* for a Rh/CeO_2 catalyst (17), by lowering the adsorption temperature the rate of H_2 spillover over the support becomes negligible and a reliable H/Rh value can be measured. Our recent measurements suggested the validity of this methodology also for these $Rh/CeO_2{-}ZrO_2$ mixed oxides (14).

NO Reduction by CO: Catalytic Activity of Reduced Fresh Catalysts and the Influence of Ageing in the Presence of NO and CO

The activity of the Rh-loaded $Ce_xZr_{1-x}O_2$ (x = 0.4, 0.5, 0.6) in the reduction of NO using CO as reductant was investigated in a flow reactor as described in the experimental section. The fresh catalysts were reduced in H_2 at 473 for 2 h before testing the catalytic activity. A typical reaction profile as a function of temperature is reported for the reduced fresh $Rh/Ce_{0.6}Zr_{0.4}O_2$ in Fig. 1. Similar behaviour is observed also for the other catalysts. At variance with the typical light-off behaviour of supported Rh catalysts, the conversion versus temperature curve of the reduced fresh $Rh/Ce_{0.6}Zr_{0.4}O_2$ shows a noticeable increase of both NO

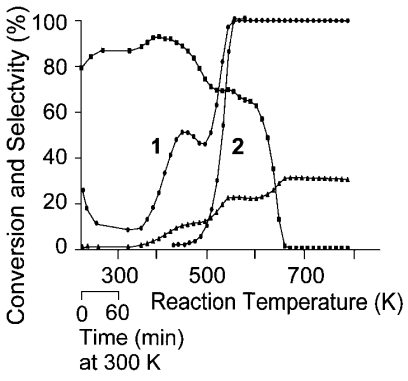

FIG. 1. NO conversion profile vs temperature for NO/CO reaction after an initial period of 60 min at 300 K on $Rh/Ce_{0.6}Zr_{0.4}O_2$: (■) Selectivity in N_2O formation and (▲) CO conversion measured on a freshly reduced catalyst; (●) NO conversion measured in (**1**) run-up experiment on a freshly reduced catalyst, (**2**) run-down experiment on an aged catalyst. Reaction conditions: weight of catalysts 50 mg, total flowrate 40 ml min^{-1}; CO (3%), NO (1%) in He, heating/cooling rate 1 K min^{-1}.

and CO conversions at low temperatures peaking at about 470 K. Upon increasing further the temperature, the conversion increases again, reaching 100% above 600 K. The conversion of CO follows a different pattern; besides the peak/shoulder at 470 K, an additional peak/shoulder is observed at about 550 K which is associated with the change of selectivity in the NO conversion from N_2O formation to give N_2 as main product. The peak at 470 K in the NO conversion is no longer observed when the catalyst, aged in the NO/CO mixture above 500 K, is immediately recycled in a run-up or run-down experiment. In this case, a typical light-off behaviour is observed as shown for the NO conversion in Fig. 1, trace 2. Apparently, the low temperature "active" state of the catalyst is destroyed upon increasing the temperature in the reaction conditions above 500 K. However, when the catalysts is re-reduced in H_2 at 473 K, the low temperature "active" state is regenerated and the reaction versus temperature profile equals that reported in Fig. 1. This experiment indicates that new sites that are active at low temperatures are generated in the catalyst upon reduction and that they undergo a reversible deactivation above 500 K. It is worth noting the conversion of NO occurring at room temperature before the catalyst was heated up in the flow of reactants. In these conditions no measurable CO conversion is observed and no O_2 is detected in the effluents of the reactor, which indicates that NO is decomposed at the expense of a concurrent oxidation of the support. We recall that before the experiment the catalyst was reduced at 473 K for 2 h.

The presence of Ce^{3+} in the support after reduction at 473 K and its oxidation to give Ce^{4+} is confirmed by *in situ* XANES spectra taken at the Ce L_{III} edge on the $Rh/Ce_{0.5}Zr_{0.5}O_2$ catalyst (Fig. 2). The calcined $Rh/Ce_{0.5}Zr_{0.5}O_2$ (Fig. 2, spectrum 1) shows a typical Ce L_{III} absorption edge of a pure Ce(IV) compound with three distinct lines denoted A, B_2, and C, respectively. With the resolution here employed, a structure B_1 appears as a shoulder of the intense B_2 line. Attribution of these lines have been discussed in detail ((18) and Refs. therein). The Ce(III) state is characterised by a white line denoted B_0 which is observed regardless of the nature of the Ce(III) compound. This line is shifted to higher energy by 1.85 eV from the B_1 line. Upon reduction at 473 K of the calcined sample, substantial amount of Ce^{3+} is formed as shown by the appearance of the B_0 line in spectrum 2 of Fig. 2. A quantitative evaluation of the amount of the Ce^{3+} present, carried out by deconvolution and fitting the Ce^{4+}/Ce^{3+} XANES spectra as described in Ref. (18), gives a value of 40%. This value is in excellent agreement with the value of 39% evaluated from the TPR of the $Rh/Ce_{0.5}Zr_{0.5}O_2$. A room temperature treatment of the reduced sample in flow of NO and CO causes a substantial oxidation of the sample as detected by the decrease of intensity of the B_0 line. After two hours of reaction, a residual amount of about 10% of Ce^{3+} is evaluated (Fig. 2, spectrum 3). Upon heating up to 473 K in the flow of NO and CO, support oxidation proceeds further to obtain the spectrum 4 of Fig. 2 which is very similar to that of the starting sample. Quantitative evaluation indicates that no Ce^{3+} is present after such treatment. It should be noted, however, that due to the ovelapping of the Ce^{3+} white line with the Ce^{4+} features, the reliability of this method for amounts of Ce^{3+} smaller than 5% is quite poor (18).

The reaction rates were measured in steady state conditions after 6–8 h of reaction at 473 K over both fresh reduced and aged (see below) catalyst. Typically, reduced fresh

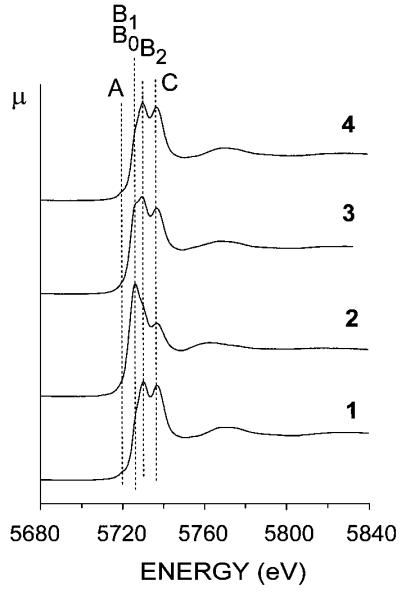

FIG. 2. *In situ* XANES spectra of (**1**) fresh $Rh/Ce_{0.5}Zr_{0.5}O_2$, (**2**) $Rh/Ce_{0.5}Zr_{0.5}O_2$ reduced in H_2 at 473 K for 2 h, (**3**) $Rh/Ce_{0.5}Zr_{0.5}O_2$ from (**2**), treated in NO–CO at 295 K for 2 h, (**4**) $Rh/Ce_{0.5}Zr_{0.5}O_2$ from (**3**), treated in NO–CO at 473 K for 2 h.

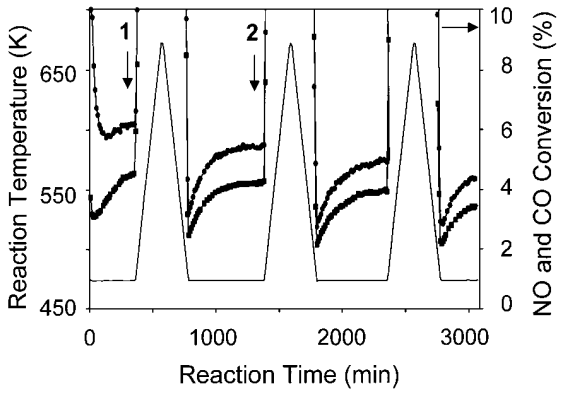

FIG. 3. The effects of thermal cycles up to 773 K and ageing at 473 K in NO–CO mixture on the (●) NO and (■) CO conversions on $Rh/Ce_{0.5}Zr_{0.5}O_2$ reduced at 1073 K. Reaction conditions: weight of catalysts 50 mg, total flowrate 40 ml min^{-1}; CO (1%), NO (1%) in He, heating/cooling rate 1 K min^{-1}. Points corresponding to the activity of (**1**) "fresh" and (**2**) partially deactivated catalyst (compare text).

catalysts show a high initial activity, which slowly (4–6 h) decreases to a stationary value. An initial decrease of catalytic activity is generally observed over supported Rh catalysts (15, 19); however, compared to Rh/Al_2O_3, a strongly enhanced NO conversion is initially observed over the reduced $Rh/Ce_{0.5}Zr_{0.5}O_2$: after 5 min on-stream at 473 K (reaction conditions as reported in Fig. 3), NO conversions of 6 and 70% are observed respectively for Rh/Al_2O_3 and $Rh/Ce_{0.5}Zr_{0.5}O_2$. Consistent with the experiment shown in Fig. 1, the NO conversion initially exceeds that of CO due to an initial NO conversion occurring partly at the expense of a Ce^{3+} oxidation. No oxygen is detected in the outlet of the reactor.

The steady state activity of the reduced fresh $Rh/Ce_{0.5}Zr_{0.5}O_2$ is more than threefold higher than that of either Rh/Al_2O_3 or aged catalyst, confirming the presence of a low temperature "active" state of the catalyst. The steady state data obtained on a reduced fresh (473 K) Rh/CeO_2, $Rh/Ce_{0.6}Zr_{0.4}O_2$, and $Rh/Ce_{0.4}Zr_{0.6}O_2$ catalysts are also included in Table 1. The consistency of both the reaction rates and activation energies measured on the Rh/CeO_2–ZrO_2 samples shows that, in the range of the compositions investigated, the modification of the catalytic activity compared to Rh/Al_2O_3 should be associated with the presence of *ceria* in the mixed CeO_2–ZrO_2 oxide rather than to a particular composition of this type of oxides. Accordingly, the high surface area Rh/CeO_2 (surface area 194 $m^2\ g^{-1}$) shows the same kind of phenomena, e.g. initial oxidation of the prereduced support and the presence of a low temperature "active state" which is reversibly deactivated under NO–CO mixture (Table 1).

The catalytic behaviour of the $Rh/Ce_{0.5}Zr_{0.5}O_2$ and the effects of ageing in NO and CO and of various treatments

TABLE 1

Reaction Rates and Apparent Activation Energies Observed over Rh/Al_2O_3, Rh/CeO_2, and $Rh/Ce_xZr_{1-x}O_2$ (x = 0.4–0.6) Catalysts

Run[a]	Catalyst	Pretreatment	Reaction rate[b] ($\times 10^9$)	Activation energy[c] (kJ mol^{-1})	
				Run up	Run down
1	Rh/Al_2O_3	H_2, 473 K, 2 h	70	115	121
2		NO + CO, 473–773 K	32	134	131
3	Rh/CeO_2	H_2, 473 K, 2 h	1120	—	96
4		NO + CO, 473–773 K	83	89	122
5		H_2, 1073 K, 2 h	130	57	118
6		NO + CO, 473–773 K	97	81	118
7	$Rh/Ce_{0.4}Zr_{0.6}O_2$	H_2, 473 K, 2 h	331	67	93
8		NO + CO, 473–773 K	90	85	87
9	$Rh/Ce_{0.6}Zr_{0.4}O_2$	H_2, 473 K, 2 h	336	67	86
10		NO + CO, 473–773 K	46		
11	$Rh/Ce_{0.5}Zr_{0.5}O_2$	H_2, 473 K, 2 h	224	66	87
12		NO + CO, 473–773 K	117	118	138
13		NO + CO, 473–773 K[d]	25	129	139
14		H_2, 473 K, 2 h	27	120	146
15		O_2, 700 K, 0.5 h, H_2, 473 K, 2 h	43	123	129
16		O_2, 700 K, 0.5 h, H_2, 1073 K, 2 h	179	86	106
17		NO + CO, 473–773 K	157	92	110
18		NO + CO, 473–773 K[c]	124	94	113

[a] Reaction conditions as reported in Fig. 1 (runs 1–10) and Fig. 3 (runs 11–18).
[b] Moles of NO converted (g catalysts)$^{-1}$ s^{-1}, measured in steady-state conditions at 473 K.
[c] Measured during the run-up/run-down cycles in the range of temperatures 473–530 K. Conversions <20%, Standard deviation ±8 kJ mol^{-1}.
[d] Aged catalyst.

were examined in detail (Table 1). Typically, after the initial pretreatment in H_2, the catalyst was aged at 473 K in a NO/CO mixture for 8 h and then the *steady state* activity was measured (here-in-after, this activity is indicated as that of a "fresh" catalyst, Table 1, runs 1, 3, 7, 9, 11). Afterwards, the catalysts were subjected to a thermal cycle such as depicted in Fig. 3, in the presence of the reactants up to 773 K (heating/cooling rate 1 K min^{-1}). The apparent activation energies for NO and CO were measured during both run-up and run-down part of the thermal cycle. After the first thermal cycle, the catalysts were allowed to react at 473 K for a further 8 h before the activity of the "partially deactivated" catalyst was measured (Table 1, runs 2, 4, 8, 10, 12). The activation energies were then measured as above-described. To investigate the long-term activity, in some experiments such thermal cycles were repeated several times. This system is indicated as "aged" catalyst in Table 1. Generally speaking, the active state of the catalyst generated by the initial reduction at 473 K slowly decays upon thermal cycles in the presence of NO and CO (Table 1, runs 11–13). Reaction rates were measured on the aged catalyst at 473 K by varying the pressure range 7–25 Torr both for the NO and CO. The data were fitted to a power type law:

$$\text{Rate (NO conversion)} = k_{NO} p(NO)^m p(CO)^n.$$

The following values were obtained: $k_{NO} = 3.2 \pm 0.5\ 10^{-8}$ ml $g^{-1}_{catalyst}$ s^{-1}, $m = -0.20 \pm 0.07$, $n = 0.24 \pm 0.02$. For comparison, Pande and Bell reported for the same reaction values of m varying between −0.37 and −0.15 and n varying between 0.04 and 0.08 for Rh supported on SiO_2, Al_2O_3, MgO (20).

Noticeably, the reduction at 473 K of the aged catalyst is no longer effective to recover the initial high activity of the fresh catalyst (Table 1, run 14). Formation of some carbon deposits on the catalyst in the reaction conditions should be discarded as a cause of the deactivation since oxidation at 700 K and subsequent reduction at 473 K does not significantly modify the behaviour of the aged catalyst (Table 1, run 15). On the contrary, after the reduction at 1073 K of the aged $Rh/Ce_{0.5}Zr_{0.5}O_2$, the initial high activity comparable to that of the "fresh" catalyst is recovered (Table 1, run 16). The reduction at 1073 K strongly modifies the behavior of the catalyst in the thermal cycles previously described. Also, in this case a partial deactivation is induced by the thermal cycles; however, upon decreasing the reaction temperature to 473 K, a slow, partial reactivation of the catalyst is observed as illustrated in Fig. 3. The activation energy for NO conversion measured during the run-up is about 86–94 kJ mol^{-1} in subsequent thermal cycles (Table 1, runs 16–18). Noticeably, the light-off temperatures for NO conversion slowly increased by about 35 K, both for the run-up and run-down experiments with the aging of the catalyst. However, upon oxidation at 700 K and subsequent reduction at 1073 K, the light-off temperatures appeared fairly constant with values similar to those observed over the fresh catalyst (Fig. 4).

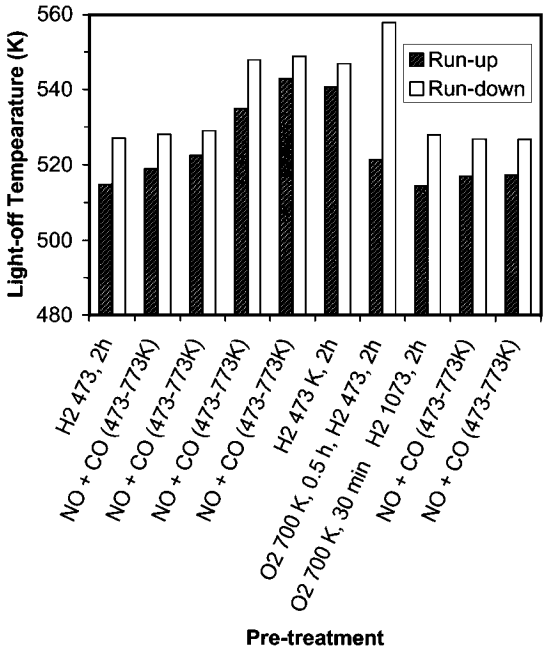

FIG. 4. The effects of thermal cycles up to 773 K and ageing at 473 K in NO–CO mixture on light-off temperatures for NO conversion of $Rh/Ce_{0.5}Zr_{0.5}O_2$ reduced at 473 and 1073 K. Reaction conditions as reported in Fig. 3.

Summarising, reduction in H_2 at 473 K of the Rh supported on CeO_2–ZrO_2 generates an "active" state of the catalyst which slowly decays with time on stream in the NO/CO mixture. However, this active state can be regenerated upon reduction at 1073 K. Moreover, this treatment makes the active state more resistant towards the ageing of the catalyst. In comparison, the NO conversion over Rh/CeO_2 decreases by about one order of magnitude after this treatment.

The values for the apparent activation energies reported in Table 1 were averaged over the entire range of temperature (473–530 K) considered. It should be noted, however, that in the run-up experiments which were carried out after the catalysts was subjected to reaction conditions for at least 6–8 h, two regions, characterised by distinct activation energy, were observed in some experiments. This is consistent with previous observation that on highly dispersed Rh/Al_2O_3 catalysts two regions characterised by distinct activation energies were observed (15). The presence of two kinetic regimes was associated with a shift of the rate-limiting step for the NO–CO reaction at high temperatures (3) and references therein. Recent evidence suggests that, in the case of Rh/Al_2O_3, it is best attributed to a variation of rhodium particle morphology due to the occurrence of particle agglomeration/disruption processes induced by CO (15).

TABLE 2

Apparent Activation Energies Measured in Steady-State Conditions over $Rh/Ce_{0.5}Zr_{0.5}O_2$

Pretreatment	Range of temperature (K)	Activation energy (kJ mol^{-1})[a] NO	CO	N_2	N_2O
H_2, 473 K	471–497 K	82	52	104	77
	497–526 K	125	111	126	124
H_2, 1073 K	476–497 K	77	60	107	67
	497–517 K	138	125	129	142

[a] Apparent activation energy for NO and CO conversions, N_2 and N_2O formation. Standard deviation ±8 kJ mol^{-1}.

There is a noticeable decrease of the activation energies measured over the freshly reduced $Rh/Ce_xZr_{1-x}O_2$ (x = 0.4–0.6) catalysts, compared to the freshly reduced Rh/Al_2O_3. Upon ageing of the $Rh/Ce_{0.5}Zr_{0.5}O_2$ catalyst in the reaction conditions, the activation energy increases to 120–130 kJ mol^{-1}. This value is of the same order of that observed over the Rh/Al_2O_3.

This increase of the apparent activation energy appears related to the kinetics of the transformation of the catalyst in the course of the run-up/run-down experiments. Table 2 reports the apparent activation energy measured in steady state conditions over the aged $Rh/Ce_{0.5}Zr_{0.5}O_2$ catalyst. Two distinct kinetic regimes characterised by different activation energies are observed below and above approximately 500 K. It is worth noting the activation energy observed for the NO conversion below 500 K, which is comparable to that observed on both fresh and reduced (1073 K) $Rh/Ce_{0.5}Zr_{0.5}O_2$. A perusal of reported data reveals that the low activation energy observed below 500 K for NO conversion is mainly associated with the reduction of NO to give N_2O, while the activation energy for N_2 formation is somewhat higher.

To investigate whether CO-induced oxidative disruption/reductive agglomeration phenomena were present in our system, the $Rh/Ce_{0.5}Zr_{0.5}O_2$ was treated in flowing CO (2%)/Ar mixture in an *in situ* IR cell (21). The IR spectra reported in Fig. 5 reveal only the presence of Rh(I) dicarbonyl, as detected by the bands at 2080 and 2008 cm^{-1}. The occurrence of this species at both 473 and 523 K indicated that the particle morphology does not change under these conditions. Conversely, reductive agglomeration of the Rh(I) dicarbonyl to give large Rh particles was observed in an equivalent experiment using Al_2O_3 as support (15).

Temperature Programmed Oxidation and Reduction Using NO and CO as Oxidant and Reductant

In order to get further insight on the nature of the active sites formed by reduction we carried out some temperature-programmed reduction and oxidation experiments using

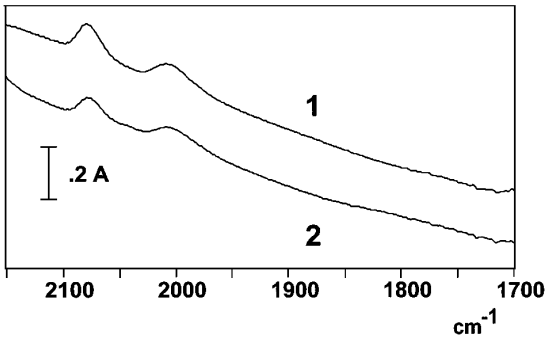

FIG. 5. *In situ* IR spectra of fresh $Rh/Ce_{0.5}Zr_{0.5}O_2$ in flow of CO (6% in He, flowrate 20 ml min^{-1}) at (**1**) 473 K and (**2**) 523 K.

CO and NO as reductant and oxidant, respectively. These experiments, in principle, allow one to investigate separately the two steps of the NO–CO reaction. The results are illustrated in Figs. 6 and 7. For comparison the TPR experiments using H_2 as reductant are shown in Fig. 8. The amount of oxygen exchanged in the TPO/TPR experiments is reported in Table 3.

The TPO of reduced (H_2, 473 and 1073 K) fresh $Rh/Ce_{0.5}Zr_{0.5}O_2$ shows a partial oxidation of the support at room temperature, while most of the oxidation occurs in

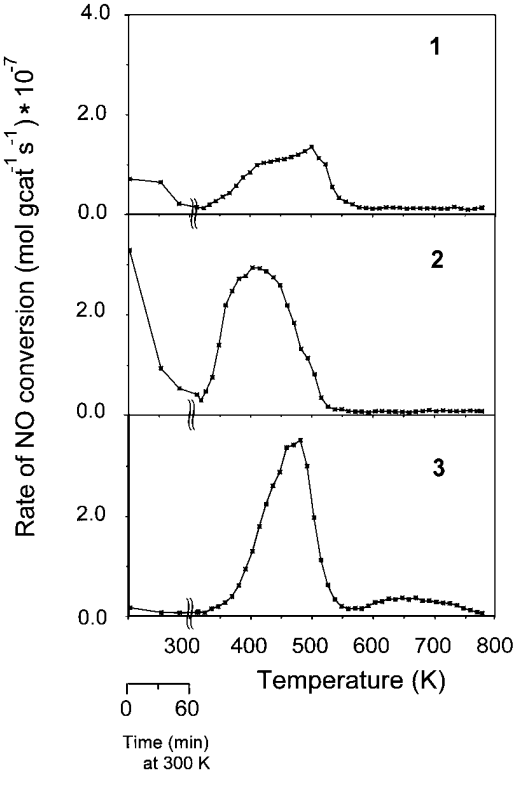

FIG. 6. Temperature programmed oxidation using NO as oxidant of (**1**) fresh $Rh/Ce_{0.5}Zr_{0.5}O_2$ reduced in H_2 at 473 K, (**2**) $Rh/Ce_{0.5}Zr_{0.5}O_2$ reduced in H_2 at 1073 K, (**3**) sample from experiment (**2**) reduced in CO at 773 K.

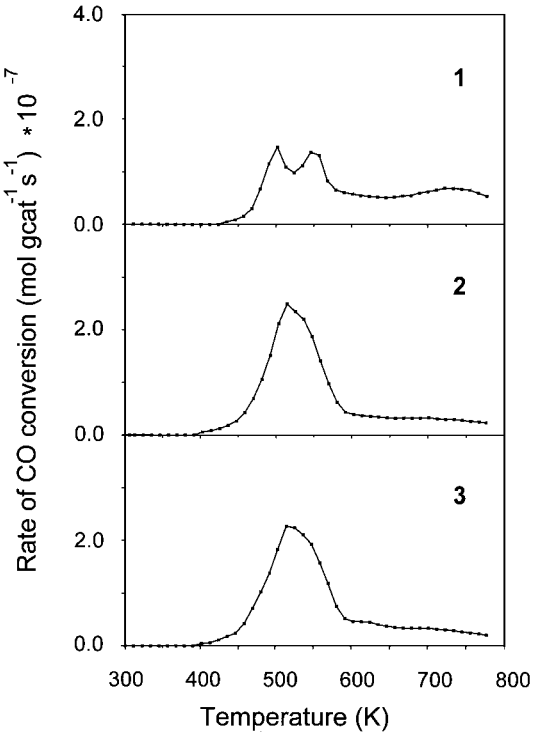

FIG. 7. Temperature programmed reduction using CO as reductant of $Rh/Ce_{0.5}Zr_{0.5}O_2$: (**1**) fresh catalyst; (**2**) catalyst reduced in H_2 at 1073 K and then oxidized in NO at 700 K; (**3**) sample from experiment (**2**) oxidized in NO at 700 K.

a single broad feature peaking at 400–470 K. The amount of exchanged oxygen depends on the temperature of reduction and it is about 1.5 fold higher after the reduction at 1073 K, compared to that at 473 K. It is worth noting that N_2O is formed almost exclusively in the TPO experiments.

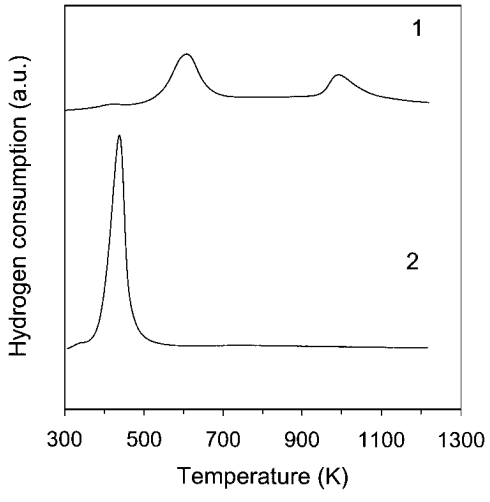

FIG. 8. Temperature programmed reduction using H_2 as reductant of $Rh/Ce_{0.5}Zr_{0.5}O_2$: (**1**) fresh catalyst; (**2**) catalyst from experiment (**1**) oxidised by pulses of O_2 (0.092 ml in Ar) at 700 K.

TABLE 3

Amount of O_2 Exchanged in the TPR/TPO Experiments

Run[a]	Experiment[b]	Pretreatment	O_2 exchanged (ml g_{cat}^{-1})
1	TPO (1)	H_2, 473 K	12
2	TPR (1)	NO, 773 K	17
3	TPO (2)	H_2, 1073 K	16
4	TPR (2)	NO, 773 K	18
5	TPO (3)	CO, 773 K	17
6	TPR (3)	NO, 773 K	18
7	TPO	NO + CO, 523 K	0.9
8	TPO	NO + CO, 473 K	Traces

[a] Sample recycled from a preceeding run, except for run 1.
[b] (1), (2), (3) values obtained in the experiments described in the corresponding curves of Fig. 6 (TPO) and Fig. 7 (TPR).

After a CO reduction, the room temperature feature of the TPO spectrum is no longer present, while the oxidation at 400–470 K appears unaffected. The TPR (CO) of the $Rh/Ce_{0.5}Zr_{0.5}O_2$, reduced in H_2 at 473 K and then oxidized in NO, shows two peaks at 480 and 570 K. A further, less intense, reduction feature appears also at 740 K. Consistently with the TPR (H_2) results, the reduction in H_2 at 1073 K modifies the reduction behaviour of the $Rh/Ce_{0.5}Zr_{0.5}O_2$; instead of the peaks at 480 and 570 K, a single strong reduction feature centred at 500 K is observed in the sintered sample and the peak at 570 K now appears as a shoulder of the peak at 500 K.

The comparison of the NO conversion profiles with the NO conversion during the NO–CO reaction is of interest. After a reduction in CO up to 773 K, the NO conversion versus temperature curves of the TPO (Fig. 6, trace 3) and the NO–CO reaction show qualitatively similar patterns from room temperature up to 500–550 K. An apparent activation energy for NO conversion of 75 kJ mol^{-1} is measured at conversions <20% for both the experiments which suggests that the same mechanism is operating in the two cases.

As shown by XANES, in the presence of NO and CO, oxidation of the Ce^{3+} sites occurs, however, residual amounts of Ce^{3+} would have escaped this technique. The presence of oxidisable species in the reaction conditions was therefore analysed by the TPO technique (Fig. 9). A sample reduced in H_2 at 1073 K and then oxidised in a TPO experiment was treated in the flow of CO and NO at 473 K until the steady state conditions were attained. After desorbing of the reactants in He flow at the reaction temperature, the sample was cooled to room temperature and subjected to a TPO run to determine the amount of the oxidisable species. The same experiment was then repeated by increasing the reaction temperature to 523 K, e.g. at a temperature where the "active" state is destroyed. Almost negligible N_2O formation is observed on the catalyst which has been treated in NO–CO at 473 K while appreciable N_2O formation occurs over the sample treated at 523 K, indicating the presence

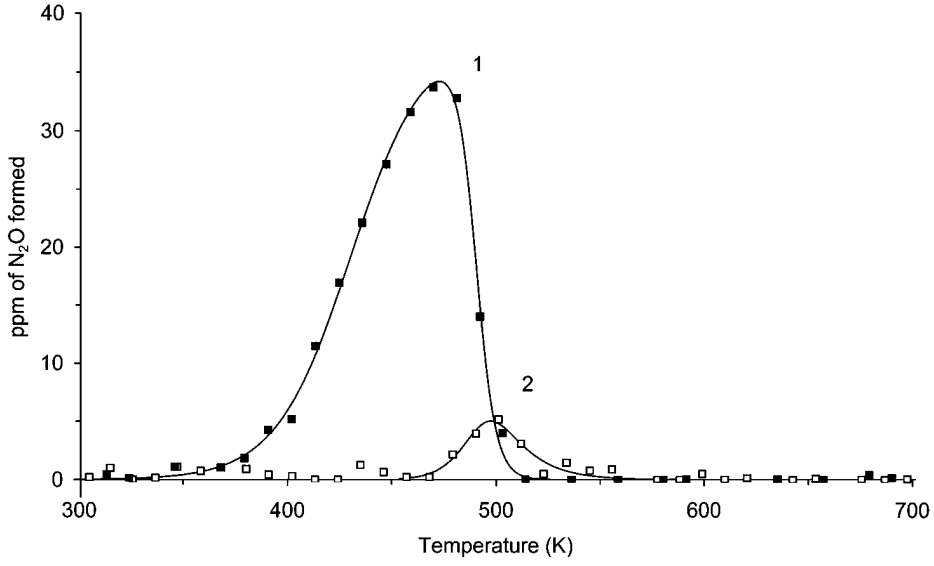

FIG. 9. Temperature programmed oxidation using NO as oxidant of $Rh/Ce_{0.5}Zr_{0.5}O_2$ subjected to NO–CO reaction at (**1**) 523 K and (**2**) 473 K.

of oxidisable species in the latter case. No reaction occurs at room temperature, suggesting that either bulk oxygen vacancies or the rhodium particles are oxidised in the TPO. As shown above, surface Ce^{3+} sites would be oxidised at room temperature.

DISCUSSION

The present data clearly are evidence of an important role of the CeO_2–ZrO_2 in modifying the catalytic activity of supported rhodium. Comparison with the Rh/Al_2O_3 discloses a strong increase of activity over the reduced fresh catalyst which is associated with the ability of the Rh/CeO_2–ZrO_2 to undergo reduction of the support at low temperatures. The reduction affects the activity mainly in three ways:

1. A strong, transient increase of NO conversion which is observed already at room temperature.
2. An "active" state of the catalyst which exists below 500 K in the reaction conditions and which is reversibly deactivated above this temperature.
3. Reduction in H_2 at 1073 K improves the durability and the reversibility of the formation of the "active" state.

As far as the first aspect is concerned, the transient increase of activity in the NO conversion is associated with a very rapid interaction of NO with oxygen vacancies generated by the reduction with the consequent oxidation of Ce^{3+} sites. As shown by previous work, reduced ceria containing moieties are easily oxidised by weak oxidants such as CO_2, H_2O, and NO (22, 23). The Ce^{4+}/Ce^{3+} redox couple interacts with NO, giving mainly N_2O, even if some formation of N_2 is observed at the initial stage of reaction (Fig. 1). In agreement with previous observations, the driving force for this initial rapid process appears to be the presence of oxygen vacancies in the bulk (10). Upon interaction with NO, the surface is rapidly oxidized and a gradient of oxygen vacancies from the bulk to the surface is generated. Under the effects of the gradient, oxygen vacancies are forced to migrate out from the bulk of the solid solution, creating new sites on the surface for further NO reduction. This is supported by the XANES measurements, even if we cannot fully discriminate on its basis whether the oxidation occurs at room temperature on the surface only or also in the bulk. Generally speaking, XANES is a bulk-sensitive technique; however, in the presence of a relatively large surface area, also, the contribution of the surface cannot be disregarded. Oxidation in the bulk of a reduced $Rh/Ce_{0.6}Zr_{0.4}O_2$ of low surface area solid solution occurred at 490 K (10). In contrast, a complete oxidation of a high surface CeO_2 occurred at room temperature (22). It appears that in the high surface area $Rh/Ce_{0.5}Zr_{0.5}O_2$, the presence of defects favours a partial oxidation in the bulk, even at room temperature.

The presence of defective structure in the high surface area sample is substantiated by the density measurements. Using a He pychnometer a density of 6.40 g ml^{-1} was measured which is lower than the value 6.80 g ml^{-1} calculated from the XRD data. When the sample is sintered, the oxidation in the bulk is hindered and it occurs at higher temperatures. Temperature-programmed oxidation using NO as oxidant supports this idea since we observed for a $Rh/Ce_{0.6}Zr_{0.4}O_2$ sample sintered to obtain a surface area of about 10 $m^2\,g^{-1}$ that the oxidation was split in two processes occurring at room temperature and 490 K.

As shown by the XANES spectra, most of the oxygen vacancies have been annihilated after interaction with NO at room temperature, leading to Ce^{3+} oxidation. A fully oxidised sample is obtained at 473 K in the presence of CO and NO. This strongly suggests that the oxygen vacancy gradient

is not responsible for the "active" state of the catalyst (point 2). However, it should be noted that the support definitely plays an active role in the generation of this active state as is evidenced by the above-reported comparison of the observed reaction orders.

While the dependence of the reaction rate on the NO is comparable to those observed for the conventional supports, the CO dependence shows a significantly higher value. Similar deviation of the pressure dependence were also observed over Rh/TiO_2 and attributed to an active role of the support in the NO–CO reaction. A possible direct participation of the support in the reaction network is substantiated by the TPR/TPO experiments. Both the TPR and TPO experiments clearly show that oxygen exchange around 400–500 K is strongly favoured on these supports. Notably, the oxidation of the reduced support occurs at lower temperatures, compared to the reduction with CO, since, with exception of the reduced fresh (473 K) $Rh/Ce_{0.5}Zr_{0.5}O_2$, the former process is almost complete by 500 K. On the contrary, the reduction using CO as reductant is peaking at about 530–550 K. This observation appears consistent with the observed pressure dependence of the reaction rate. If it is assumed that the interaction of NO with the reduced support is responsible for N_2O formation, then one could expect a positive reaction order in CO pressure, keeping in mind that the reduction of the support is less favoured, compared to the oxidation. Increasing the CO pressure, reduction of the support is favoured which allows an easy conversion of NO on the support.

The features observed in the TPR/TPO experiments deserve some further comments. The shift of the peak due to bulk oxidation with the temperature of reduction may be attributed to a different degree of reduction. Upon reduction of Ce^{4+}, the lattice parameter increases due to the higher ionic radius of Ce^{3+} (0.110 nm vs 0.097 nm). This more open structure will result in higher oxygen mobility in the bulk, accounting for the lower peak temperature after the reduction at 1073 K. It can be argued, however, that, one should expect in the subsequent TPO, e.g. that after a reduction by CO of the sintered catalyst, the same shift of the oxidation towards lower temperature compared to the H_2, 473 K-treated catalyst, since the degree of reduction is approximately the same after both the H_2, 1073-K and the subsequent CO reduction. It should be noted, however, that, even though the degree of reduction is quite similar in the two cases, there is another important difference in the TPO when H_2 and CO are used as reductant; there is no oxidation of the support occurring at room temperature when CO is used as reductant. Formation of surface carbonates during the CO reduction could easily account for the lack of surface oxidation and, perhaps, they can also account for the shift of the oxidation in the bulk towards higher temperature. Oxidation in the bulk can be viewed as a migration of bulk oxygen vacancies towards the surface of the support. The driving force for the migration of the oxygen vacancies will be then the gradient of the oxygen vacancies from the bulk to the surface. The presence of surface carbonates modifies the surface, compared to a reduction in H_2, when surface carbonates are eliminated. Oxidation of the surface is indeed hindered and consequently oxidation in the bulk would be also less easy. Heating of CeO_2 at 673 K in the presence of CO led to the formation of surface carbonates (24).

Surface carbonates could also play an important role in the progressive deactivation of the fresh catalyst. If the support is responsible for the NO conversion, then accumulation of surface carbonates may well hinder the ability of the reduced support to efficiently reduce NO.

An important observation of the present work is the enhanced catalytic activity after the reduction at 1073 K. In this regard it should be recalled that reduction at high temperatures strongly modifies the redox properties of the present $Rh/Ce_{0.5}Zr_{0.5}O_2$ catalyst (11) as exemplified in Fig. 8. We refer the reader to previous work (11) for a full discussion of this unusual reduction behaviour; however, with respect to the present results, it is worth noting that the initial TPR experiment (e.g., reduction up to 1273 K) strongly improves the reducibility of the support at low temperatures (Fig. 8, trace 2). It is also worth noting that no appreciable decrease of the oxygen uptake/release ability was detected upon repeated TPR/oxidation experiments (11). This observation is also confirmed by the present results which show a reasonable agreement between the amounts of oxygen released and accumulated respectively in the TPR and TPO experiments (Table 3). The value of 12 ml g^{-1} observed after the reduction in H_2 at 473 K is associated with an incomplete reduction of the support (compare Fig. 8). Improvement of the redox properties of the support after the reduction at 1073 K could therefore be responsible for the better performances of the $Rh/Ce_{0.5}Zr_{0.5}O_2$ catalyst at low temperatures.

In fact, attributing the formation of the active state upon reduction at 1073 K to a strong metal support interaction type of effect should be disregarded on the basis of the following observations: reduction at 1000 K decreased the H_2 chemisorption on the $Rh/Ce_{0.5}Zr_{0.5}O_2$ by about 35%; however, the observed $H/Rh = 0.20$ appears to be sufficiently high to exclude that the catalyst has entered into a deep SMSI state. Moreover, it was shown that the SMSI state is reversed in the presence of oxidants such as H_2O and CO_2 formed in the CO or CO_2 hydrogenation (25).

Also the catalytic behaviour of the Rh/CeO_2 confirms this interpretation.

Reduction of Rh/CeO_2 at 1073 K induces a strong sintering of the support, leading to a loss of redox abilities at low temperatures (14). At the same time a strong deactivation of the Rh/CeO_2 occurs (Table 1), confirming the crucial role of ZrO_2 in improving the catalytic performances.

There is another open question which needs an answer: Why the low temperature "active" state of the catalyst is reversibly deactivated above 500 K? At present we do not have a fully satisfying response to this important question; however, some suggestions can be advanced. As written above, the change of the activation energy with temperature was previously attributed to a variation of Rh particle morphology in the reaction conditions induced by CO (11). CO in this case has a dual role: above 500 K it favours aggregation of the Rh particles supported on Al_2O_3, while below 500 K it induces an oxidative disruption of Rh particles as detected by formation of the $>Rh^I(CO)_2$ species (15). The latter process is further favoured in the presence of NO. The *in situ* IR spectra of $Rh/Ce_{0.5}Zr_{0.5}O_2$ show only the presence of the rhodium dicarbonylic species in the presence of CO at both 473 and 523 K (Fig. 5). This observation rules out that Rh particle agglomeration/disruption should be responsible for the observed variation of the activation energy.

The observation of the presence of the geminal dicarbonyl at 523 K clearly suggests that the $Ce_{0.5}Zr_{0.5}O_2$ support effectively stabilises the rhodium dispersion in the reaction conditions.

The TPO experiments carried out after the catalysts has been subjected to the CO/NO mixture at 473 and 523 K may give some insight. As matter of fact, traces of oxidisable species were found after the treatment at 473 K while a significant amount was found in the other case (Fig. 9). The relatively small amount of the oxidisable species found in the latter case suggests that they can be related to surface or subsurface region of the catalyst. A facile NO conversion is observed only on the carbonate-free surface which accounts for the peak temperatures observed in Fig. 9.

The improved NO conversion below 500 K can be rationalised according to a catalytic cycle depicted in the scheme which suggests a new role both for the supported metal and support itself.

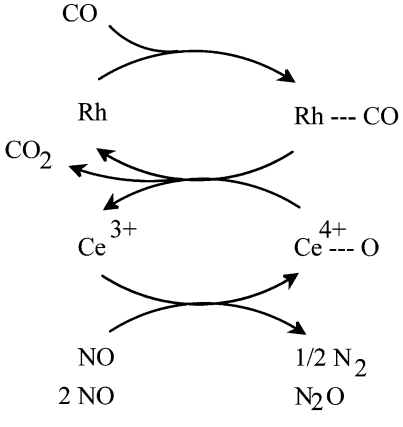

In this scheme, the NO conversion occurs at the expense of the Ce^{4+}/Ce^{3+} redox couple, while the supported metal favours creation of the oxygen vacancies by activation of the reducing agent. Immediately after the reduction, bulk oxygen vacancies appear to be involved in the transient high conversion of NO. The presence of the oxygen vacancy gradient and the carbonates free surface provide the additional driving force which allows a fast and complete oxidation of the support. Once the oxygen vacancies are filled, the durable (vide infra) "active" state of the catalyst is observed at 473 K. In these conditions, the surface or subsurface regions appear to be involved in the catalytic cycle. As a matter of fact, the positive pressure dependence on the CO pressure cannot be easily rationalised on the basis of a catalytic cycle based on Rh alone. Increase of the CO pressure should favour an increase of coverage by CO of the metal surface which would reasonably interfere both with the NO dissociation and/or N-pairing which were suggested as rate determining steps in the NO conversion on Rh (3).

As indicated by the TPO experiments, NO efficiently oxidises the reduced support below 500 K, and consistently, traces of oxidisable species were detected after the NO–CO reaction at 473 K. On the contrary these species were detected after the reaction at 523 K, suggesting a reduced state of the $Ce_{0.5}Zr_{0.5}O_2$ surface in NO/CO at 523 K. According to this observation, the "active" state of the catalysts is present as long as the reduced surface is able to interact with the NO and reduce it to N_2O, e.g. below 500 K. Above 500 K, reduction of NO which refills surface oxygen vacancies is no longer effective due to the high lability of the surface oxygens. According to this model the driving force for NO reduction is related to the stability of the surface oxygen vacancies according to the equilibrium:

$$2Ce^{3+} + V_s^{\cdot\cdot} + 1/2O_2 \rightleftharpoons 2Ce^{4+} + O_s,$$

where $V_s^{\cdot\cdot}$ and O_s indicate respectively surface oxygen vacancy and surface oxygen.

Below 500 K, the equilibrium would be shifted to the right which provides the driving force for the reduction of NO. Above 500 K, the equilibrium is shifted to the left and the catalytic cycle mediated by CeO_2–ZrO_2 is deactivated. On the basis of the present results, it cannot be discerned if only the surface is involved in the "active" state of the catalysts or whether near-surface sites participate as well. The high activity of the catalyst after the reduction at 1073 K suggests that the subsurface region may be involved. Upon a reduction at 1000 K of the $Rh/Ce_{0.5}Zr_{0.5}O_2$ the surface area decreased from 53 $m^2\,g^{-1}$ to 18 $m^2\,g^{-1}$ which reasonably should induce a partial deactivation of the catalyst. In agreement, long-range effects have been recently invoked to explain the participation of the lattice oxygens in the oxidation of CO over a Rh/CeO_2 catalyst (26).

In conclusion, the present work discloses twofold effects of a reduction in H_2 on the catalytic activity of

$Rh/CeO_2–ZrO_2$ catalysts in the reduction of NO by CO: (i) highly productive transient NO conversion which is associated with an oxidation in the bulk of the reduced support; (ii) an "active" low-temperature state of the catalysts which is associated with the ability of the support to promote NO reduction.

Furthermore, the stability of the $Rh/Ce_{0.5}Zr_{0.5}O_2$ against deactivation upon sintering is evidenced which makes these systems very attractive for any catalytic redox process demanding high thermal stability.

ACKNOWLEDGMENTS

Professor Gilberto Vlaic, Dr. Gabriele Balducci, and Dr. Roberta Di Monte are acknowledged for helpful discussions. Magneti Marelli, D.S.S., CNR (Rome), The Ministero dell'Università e della Ricerca Scientifica—MURST 40% (Rome) and Università di Trieste are acknowledged for financial support.

REFERENCES

1. Taylor, K. C., "Catalysis-Science and Technology" (J. R. Anderson and M. Boudart, Eds.), Chap. 2. Springer-Verlag, Berlin, 1984.
2. Taylor, K. C., *Catal. Rev.-Sci. Eng.* **35**, 457 (1993).
3. Shelef, M., and Graham, G. W., *Catal. Rev.-Sci. Eng.* **36**, 433 (1994).
4. Crucg, A. (Ed.), *in* "Catalytic Automotive Pollution Control II," *Stud. Surf. Sci. Catal.*, Vol. 71, p. 125. Elsevier, Amsterdam, 1991.
5. Oh, S. H., *J. Catal.* **124**, 477 (1990).
6. Golunski, S. E., Hatcher, H. A., Rajaram, R. R., and Truex, T. *J., Appl. Catal. B-Environ.* **5**, 367 (1995).
7. Nunan, J. G., Robota, H. J., Cohn, M. J., and Bradley, S. A., *J. Catal.* **133**, 309 (1992).
8. Fornasiero, P., Di Monte, R., Ranga Rao, G., Kaspar, J., Meriani, S., Trovarelli, A., and Graziani, M., *J. Catal.* **151**, 168 (1995).
9. Ranga Rao, G., Kaspar, J., Di Monte, R., Meriani, S., and Graziani, M., *Catal. Lett.* **24**, 107 (1994).
10. Ranga Rao, G., Fornasiero, P., Di Monte, R., Kaspar, J., Vlaic, G., Balducci, G., Meriani, S., Gubitosa, G., Cremona, A., and Graziani, M., *J. Catal.* **162**, 1 (1996).
11. Fornasiero, P., Balducci, G., Di Monte, R., Kaspar, J., Sergo, V., Gubitosa, G., Ferrero, A., and Graziani, M., *J. Catal.* **164**, 173 (1996).
12. Balducci, G., Fornasiero, P., Di Monte, R., Kaspar, J., Meriani, S., and Graziani, M., *Catal. Lett.* **33**, 193 (1995).
13. Meriani, S., and Soraru, G., "Ceramic Powders" (P. Vicenzini, Ed.), pp. 547–554. Elsevier, Amsterdam, 1983.
14. Fornasiero, P., Kaspar, J., and Graziani, M., *J. Catal.* **167**, 576 (1997).
15. Kaspar, J., de Leitenburg, C., Fornasiero, P., Trovarelli, A., and Graziani, M., *J. Catal.* **146**, 136 (1994).
16. Yashima, M., Arashi, H., Kakihana, M., and Yoshimura, M., *J. Amer. Ceram. Soc.* **77**, 1067 (1994).
17. Bernal, S., Calvino, J. J., Cifredo, G. A., Gatica, J. M., Omil, J. A. P., and Pintado, J. M., *J. Chem. Soc. Faraday Trans.* **89**, 3499 (1993).
18. El Fallah, J., Boujana, S., Dexpert, H., Kiennemann, A., Majerus, J., Touret, O., Villain, F., and Le Normand, F., *J. Phys. Chem.* **98**, 5522 (1994).
19. Hecker, W. C., and Bell, A. T., *J. Catal.* **84**, 200 (1983).
20. Pande, N. K., and Bell, A. T., *J. Catal.* **98**, 7 (1986).
21. Zorzut, M., Doctorate thesis, University of Trieste, 1996.
22. Padeste, C., Cant, N. W., and Trimm, D. L., *Catal. Lett.* **28**, 301 (1994).
23. Trovarelli, A., Dolcetti, G., de Leitenburg, C., Kaspar, J., Finetti, P., and Santoni, A., *J. Chem. Soc. Faraday Trans.* **88**, 1311 (1992).
24. Badri, A., Lamotte, J., Lavalley, J. C., Laachir, A., Perrichon, V., Touret, O., Sauvion, N. S., and Quemere, E., *Eur. J. Solid State Inorg. Chem.* **28**, 445 (1991).
25. Trovarelli, A., Mustazza, C., Dolcetti, G., Kaspar, J., and Graziani, M., *Appl. Catal.* **65**, 129 (1990).
26. Bunluesin, T., Cordatos, H., and Gorte, R. J., *J. Catal.* **157**, 222 (1995).